Industrial Application of Topology Optimization for Combined Conductive and Convective Heat Transfer Problems

Zhou, Mingdong; Alexandersen, Joe; Sigmund, Ole; Pedersen, Claus B. W.

Published in:
Structural and Multidisciplinary Optimization

Link to article, DOI:
10.1007/s00158-016-1433-2

Publication date:
2016

Document Version
Peer reviewed version

Noname manuscript No.
(will be inserted by the editor)

Industrial Application of Topology Optimization for Combined Conductive and Convective Heat Transfer Problems

Mingdong Zhou [a,b] · **Joe Alexandersen** [b] · **Ole Sigmund** [b] · **Claus B.W. Pedersen** [c]

Received: date / Accepted: date

Abstract This paper presents an industrial application of topology optimization for combined conductive and convective heat transfer problems. The solution is based on a synergy of computer aided design and engineering software tools from Dassault Systèmes. The considered physical problem of steady-state heat transfer under convection is simulated using SIMULIA-Abaqus. A corresponding topology optimization feature is provided by SIMULIA-Tosca. By following a standard workflow of design optimization, the proposed solution is able to accommodate practical design scenarios and result in efficient conceptual design proposals. Several design examples with verification results are presented to demonstrate the applicability.

Keywords Topology optimization · Industrial application · Conductive and Convective heat transfer

1 Introduction

Topology optimization is a generative design tool for conceptual structural design, pushing the limit of product performance based on computer simulation and optimization technologies. It originates from the area of mechanical structural design (Bendsøe and Kikuchi (1988); Bendsøe and Sigmund (2003)) (e.g. aircraft, automotive, etc.) where a lightweight structural layout is desired that satisfies static or dynamic design requirements. It now has been broadened to industrial application for multi-disciplinary problems.

[a] Dassault Systèmes Germany GmbH, SIMULIA Office, Albert-Nestler-Str.17, 76131 Karlsruhe, Germany
[b] Solid Mechanics, Department of Mechanical Engineering, Technical University of Denmark, Nils Koppels Alle, Building 404, DK-2800 Kgs. Lyngby, Denmark
E-mail: minzho@mek.dtu.dk
[c] Dassault Systèmes Germany GmbH, Südportal 1, Nordport Towers, 22848 Germany
E-mail: Claus.PEDERSEN@3ds.com

Accepted - to be published in SMO (Structural and Multidisciplinary Optimization) 2016.

This paper presents an industrial solution to design topologically optimized structures for combined conductive and convective heat transfer problems. The solution is a synergy of various technologies, including Computer Aided Design (CAD), Finite Element Analysis (FEA) and topology optimization, which are enabled by Dassault Systèmes softwares Catia, SIMULIA-Abaqus (2015) and SIMULIA-Tosca (2015), respectively. The proposed solution can be applied to the industrial design of electronic devices, heating appliances, combustion engines and electric motors etc., when thermal management becomes critical besides other design requirements such as low weight, high stiffness and strength.

The considered physical problem herein is steady-state heat transfer under convection where thermal energy is transferred through (i) conduction inside the structural body and (ii) convection across the structure-fluid interface. For topology optimization of such a problem, one key issue is to characterize the convection load in the optimization process. With the density based topology optimization approach, the convection surface is loosely defined at the beginning and constantly changing once the overall topology has been settled. Since convection is a surface controlled phenomenon, it is important to find a way to effectively interpolate the convection into the design-domain. In previous research, various ways have been proposed to model the convection: Sigmund (2001) uses a simplified convection model where side convection is indirectly modeled by conduction into void regions; Yin and Ananthasuresh (2002) use a density-based peak interpolation function; Yoon and Kim (2005) introduce a special type of parameterized connectivity between elements; Bruns (2007) suggests to interpolate the convection coefficient (also known as film coefficient) as a function of the density-gradient; Iga et al (2009) use a density-based smeared-out Hat-function, which also tried to take variation in the strength of the convective heat transfer into account; Dede et al (2015) adopt a solution similar to Iga et al (2009) to design and manufacture heat sinks subject to jet impingement cooling including spatial variability of the convection coefficient. Another approach is level set method based optimization(Ahn and Cho (2010); Coffin and Maute (2015)), for which the convection is defined precisely at the structure-fluid interface.

The topology optimization feature for combined conductive and convective heat transfer problems in SIMULIA-Tosca follows the idea which is initially suggested by Bruns (2007) and investigated by Alexandersen (2011a,b). A simplified engineering approach is adopted by assuming a design-dependent film coefficient in the optimization process, which is readily compatible with the thermal analysis in SIMULIA-Abaqus. It should be mentioned that it is possible to apply topology optimization to the full conjugate heat transfer problem (see Yoon (2010) for forced convection and Alexandersen et al (2014) for natural convection). However, this increases the computational cost significantly and is currently not desirable in industrial settings.

The remaining content of this paper is organized as follows. In Chapter 2, the governing equation and finite element model of steady-state heat transfer under convection are first introduced. Then, the importance of applying

a design-dependent convection in topology optimization is highlighted using a demonstration example. In addition, an industrial workflow of design optimization using CAD and CAE softwares is stated. In Chapter 3, several industrial design examples are presented and discussed with verification results. Conclusions are stated in Chapter 4.

2 Problem Formulation

2.1 Steady-state heat transfer under convection

The governing equation for the computational domain Ω is the steady-state heat transfer equation:

$$-\frac{\partial}{\partial x_i}\left(k\frac{\partial T}{\partial x_i}\right) = 0 \text{ in } \Omega, \tag{1}$$

where T is the temperature field, x_i are the spatial coordinates and k is the thermal conductivity. The boundary is split into disjoint subsets $\Gamma = \Gamma_{\text{flux}} \cup \Gamma_{\text{ins}} \cup \Gamma_{\text{conv}} \cup \Gamma_{\text{dir}}$, on which the following boundary conditions are imposed:

$$-k\frac{\partial T}{\partial x_i}n_i = q_0 \qquad \text{on } \Gamma_{\text{flux}}, \tag{2}$$

$$-k\frac{\partial T}{\partial x_i}n_i = 0 \qquad \text{on } \Gamma_{\text{ins}}, \tag{3}$$

$$-k\frac{\partial T}{\partial x_i}n_i = h(T - T_{\text{ref}}) \qquad \text{on } \Gamma_{\text{conv}}, \tag{4}$$

$$T = T_0 \qquad \text{on } \Gamma_{\text{dir}}, \tag{5}$$

where (2) is the prescribed surface flux condition, (3) is the insulation condition, (4) is the boundary convection condition, and (5) is the prescribed temperature condition. Furthermore, q_0 is the prescribed surface flux, h is the convection coefficient, T_{ref} is the reference temperature of the ambient fluid and T_0 is the prescribed temperature.

By discretizing the governing equation using finite elements, a system of linear equations is obtained as follows:

$$(\mathbf{K} + \mathbf{H})\,\mathbf{t} = \mathbf{f} + \mathbf{f}_h, \tag{6}$$

where $\mathbf{K}$ is the conductivity matrix, $\mathbf{H}$ is the convection matrix, $\mathbf{t}$ is the vector of nodal temperatures, $\mathbf{f}$ is the flux vector arising from (2) and $\mathbf{f}_h$ is the convection vector arising from (4).

2.2 Design-dependent convection in topology optimization

Heat transfer by convection happens when solid objects are in contact with a fluid and the energy is transferred to or from a surrounding fluid across the

solid-fluid interface due to a temperature difference. Generally, the efficiency of heat transfer is determined by various factors, including the property and speed of the moving fluid and the size, shape and properties of the solid object. It is possible to simulate a conjugate heat transfer process using thermo-fluidic modeling, which can also be leveraged in topology optimization Yoon (2010); Alexandersen et al (2014)). However, it requires intensive computational resources and it is currently not desirable for industrial applications. Another simplified way to characterize the heat transfer by convection is to define an average convection heat transfer coefficient and a convective flux at the interface by (4). The convection coefficient can be estimated or found in engineering tables for different solid-fluid interactions. It is common engineering practice to simplify thermal calculations in such a way and a topology optimization approach considering this simulation approach is therefore of industrial importance.

A topology optimization feature for thermal problems is implemented in SIMULIA-Tosca. The idea is a variant of the work in (Bruns (2007); Alexandersen (2011a,b)), where both the conductivity and the convection coefficient are assumed design-dependent and interpolated during the optimization process. Due to confidentiality, implementation details are not given in this paper. However, the importance of using design-dependent convection in topology optimization is verified using a demonstration example.

As shown in Fig. 1(a), a rectangular block of dimension $250 \times 250 \times 40$mm is setup as the design domain. It is subject to a prescribed temperature $T = 100^oC$ at the central region of the left surface (red color) and a convection of a reference ambient temperature $T_{ref} = 20^oC$. The conductivity of the solid material is assumed to be $k = 0.385\text{W}/(\text{mm} \cdot \text{K})$ and the convection coefficient is $h = 10^{-5}\text{W}/(\text{mm}^2 \cdot \text{K})$. The model is discretized into $100 \times 100 \times 4$ linear hexahedral elements. The optimization objective is to maximize the reaction flux[1] at the region where prescribed temperature applies. In addition, the problem is subject to a volume constraint, which must be less or equal to 40% of the design domain. Fig. 1(b) shows the optimized density distribution[2] by using a design-independent convection, where a constant convection coefficient is assumed over the outer boundary of the design domain during the optimization. The corresponding validation result in Tab. 1 shows that it achieves a total reaction flux of 138.5W at the prescribed-temperature region. As a comparison, the optimized design with a design-dependent convection is given in Fig. 1(c). It not only shows different topology and shape from the previous design but also possesses a larger surface area and a better thermal conductive behavior with a total reaction flux of 144.2W at the prescribed-temperature region. Note, that both designs are obtained under the same optimization parameters except for the convection scheme. Thus, it can be

[1] For readers with a background of solid mechanics, the reaction flux is analogous to the reaction force when a prescribed displacement boundary condition is applied in a static mechanical problem.

[2] The color scale bar shown in Fig. 1 for the density distribution applies to all the examples in this paper.

concluded that for even the present simple heat transfer problem, by using the design-dependent convection scheme has a significant impact on both the optimized structural layout as well as the objective value.

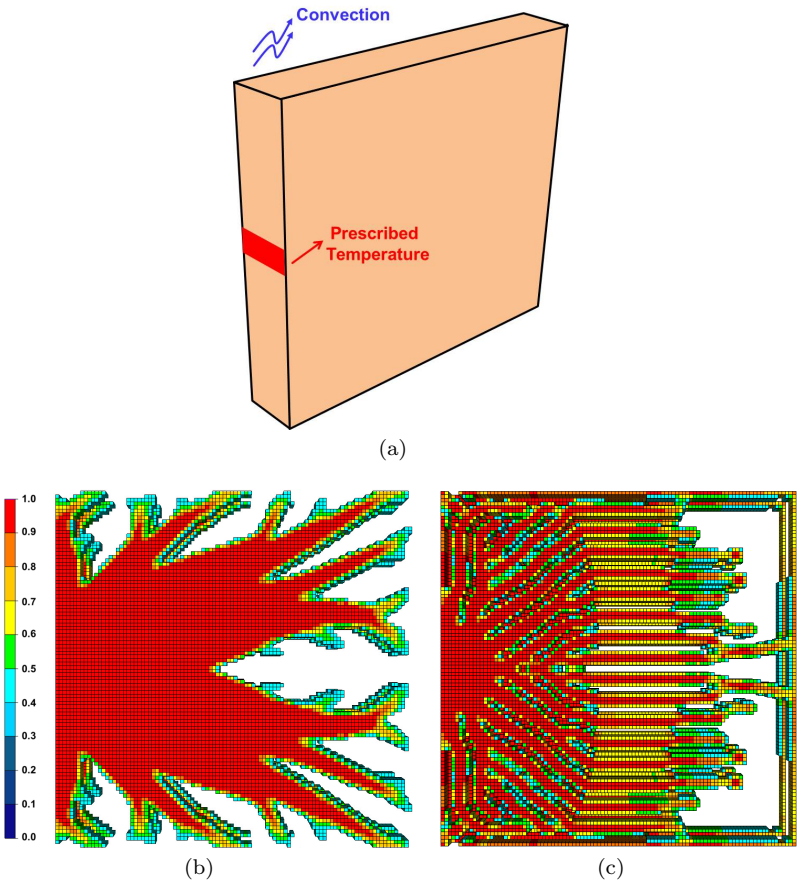

Fig. 1: Topology optimization with a constant and a design-dependent convection: (a) design domain and boundary conditions; (b) optimized density distribution using a constant and design-independent convection; (c) optimized density distribution using a design-dependent convection.

2.3 An integrated CAD and CAE workflow

The proposed solution is based on an integrated Computer Aided Design (CAD) and Engineering (CAE) workflow enabled by Dassault Systèmes. As shown in the flow chart in Fig. 2, a geometric model is initially prepared in a

Table 1: Verification of the optimized designs obtained by different convection schemes

	Constant	Design-Dependent
Total Reaction Flux (W)	138.5	144.2
Total Surface Area (mm^2)	202646	215673
Volume	40.0%	40.0%

CAD software, such as Catia or Solidworks, and then a finite element model is created in SIMULIA-Abaqus for topology optimization. Upon setting up the optimization goals and constraints with thermal related design responses, a simulation based topological design process is executed using SIMULIA-Tosca. For each design iteration, the considered problem of steady-state heat transfer under convection is simulated using SIMULIA-Abaqus. After that, the optimization module performs an adjoint sensitivity analysis and uses a gradient-based optimizer to search for an optimized design. Once the optimization process converges by satisfying certain stopping criteria, the optimized density distribution is smoothed and transferred into a CAD model. Finally, a finite element model is generated accordingly for performance verification. Downstream applications such as detailed design or further shape optimization can be performed based upon the optimized smoothed design.

3 Design Examples

The present section shows several examples demonstrating the applicability of the proposed solution. Manufacturing restrictions such as minimum member size, symmetry, casting and extrusion constraints are leveraged in the topology optimization process. The casting constraint is applied to avoid undercut along the pulling direction for casting and to prevent possible nucleation of internal holes. The latter will cause unrealistic energy loss based on the simplified engineering convection scheme considered. Note, that the optimized structure may not be castable if more than one casting constraint is used. Some key results and statistics at the workflow, including the optimized density distributions, the convergence curves, the corresponding smoothed designs and verification results are provided.

3.1 Topology optimization with different types of finite elements

One prerequisite for general industrial application of topology optimization is to support different types of finite elements. The present section demonstrates the robustness of SIMULIA-Tosca on topologically designing a heat conductor using different types of elements. The initial geometry of the model and boundary conditions are given in Fig. 3(a), where a cube is subject to a heat flux of magnitude $2.0W/mm^2$ at the central region (purple color) of

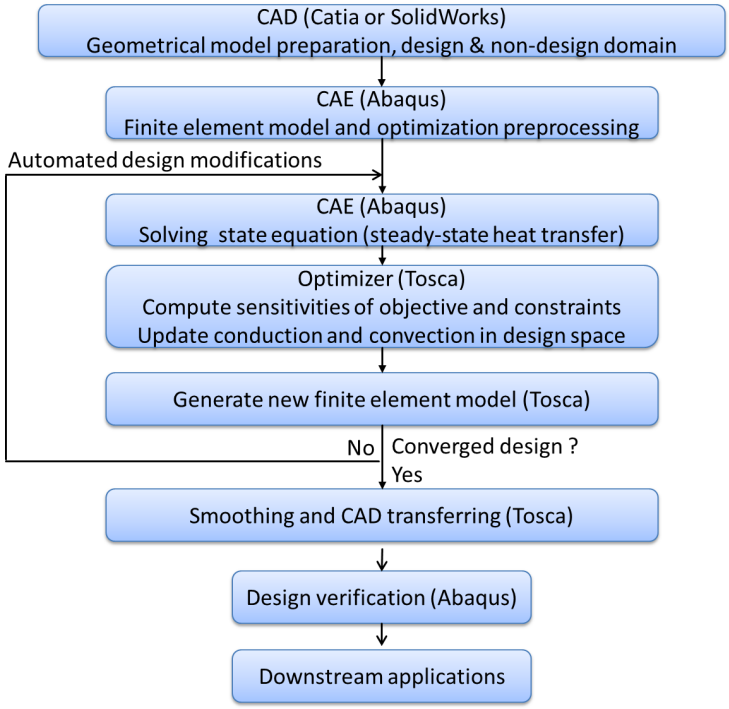

Fig. 2: Workflow of topological designing using Dassault Systèmes software solutions

the bottom surface, a prescribed temperature $T_0 = 0^oC$ at different locations (red color) on the top surface and a convection of $T_{ref} = 20^oC$ and $h = 10^{-5}\text{W}/(\text{mm}^2 \cdot \text{K})$ over the design domain (brown color). The dimension of the cube is $40 \times 40 \times 40$mm and the conductivity is $k = 0.237\text{W}/(\text{mm} \cdot \text{K})$. The design problem is to minimize the thermal compliance subject to a volume constraint of 20% of the design domain. The thermal compliance is defined as a summation of the product of the equivalent nodal heat flux and temperature values at the external-flux region. The convergence criterion is a measurement based upon (i) the change in the objective function to be less than or equal to 0.1% (ii) the change in the density to be less than 0.1% between a current and a previous optimization iteration.

The cube is discretized with four different types of finite elements, namely linear tetrahedrons (DC3D4), quadratic tetrahedrons (DC3D10), linear hexahedrons (DC3D8) and quadratic hexahedrons (DC3D20), respectively. The optimized designs are compared in Fig. 3(b-q). Each row of figures shown from left to right lists the element type, the density distribution and the smoothed designs from isometric and top views, respectively. All of the four optimizations converge to the same topology and almost the same shape. The statistics of the optimization, including the number of elements and nodes per mesh, and

Table 2: Statistics of the design in Fig. 3 and verification results

Element type	Number of Elements	Number of nodes	Average Temp. at flux regions (^oC)	Volume
DC3D8	32768	35937	81.9	20.0%
DC3D20	32768	140481	81.8	20.4%
DC3D4	130075	24663	80.3	19.4%
DC3D10	130075	185544	79.5	19.4%

verification results of the four smoothed designs using quadratic tetrahedron (DC3D10) meshes are listed in Table 2. All of the four designs have an average temperature around 80^oC at the external-flux region. The slight difference in the volume is due to postprocessing, e.g. the iso-surface cut from the density model and smoothing. The performance of the designs obtained by the tetrahedron meshes are better than those by the hexahedron meshes because more elements are applied in the optimization. The convergence curves of all designs are shown in Fig. 4, in which there are up to 10% difference in evaluating the thermal compliance between using linear and quadratic elements. Note, that two additional symmetry constraints are imposed for the tetrahedron meshes in order to ensure symmetric results as shown in Fig. 3(c-e) and (g-i). Otherwise the optimized results are slightly asymmetric due to asymmetric meshing of the design domain.

The smoothed design proposals shown in Fig. 3 exhibit a structural topology connecting the heat source to the four sinks ($T = 0^oC$) at the middle regions of the edges on the top surface. The other four heat sinks at the corners as shown in Fig. 3(a) have a longer distance from the heat source and thus, they are less efficient in energy transfer. Verification shows that only 2% of the energy is transferred through convection in this example. Hence, the problem here is conduction-dominated. Nonetheless, it demonstrates the flexibility of SIMULIA-Tosca in handling different types of finite elements and yielding consistent results irrespective upon continuum element types for heat-transfer based topology optimization .

3.2 Topological design of an electric motor cover

3.2.1 Optimized design with thermal design responses

The proposed solution is applied to design of an electric motor cover such that the heat generated from the motor can be transferred efficiently to surrounding environment. Fig. 5 shows the geometric model (a half of the E-motor cover) consisting of design and non-design domains. The model is subject to a uniform surface heat flux of magnitude 0.02W/mm^2 at the inner wall. Meanwhile a forced convection exists over the structural surface. The model has a length

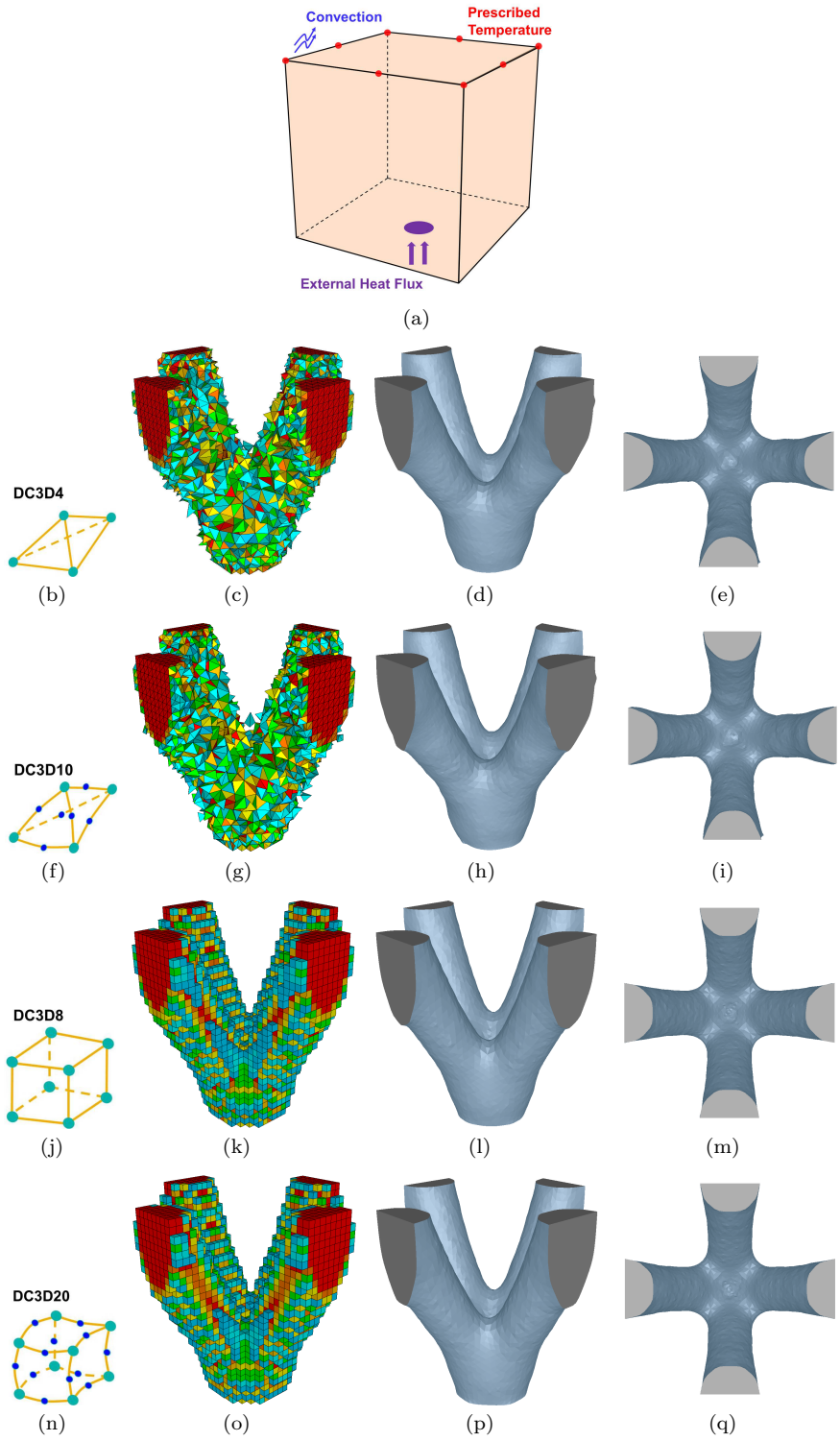

Fig. 3: Topology optimization using different types of elements: (a) boundary conditions; (b-q) (for each row from left to right) element type, optimized density distribution and smoothed designs (snapshots from different views). Element types (from top to bottom) 4-node tetrahedron (DC3D4), 10-node tetrahedron (DC3D10), 8-node linear hexahedron (DC3D8) and 20-node linear hexahedron (DC3D20), respectively.

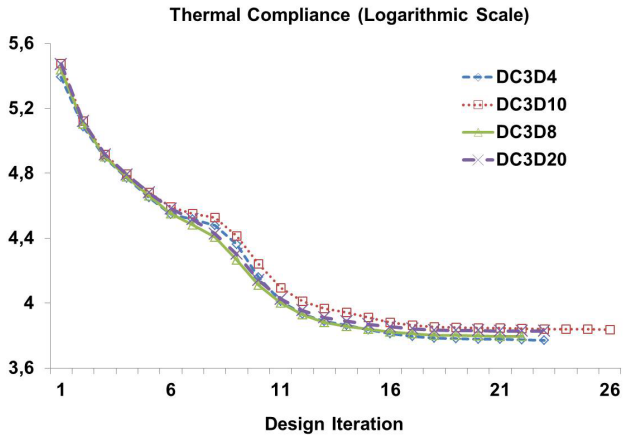

Fig. 4: Optimization convergence curves using four different element types as shown in Fig. 3

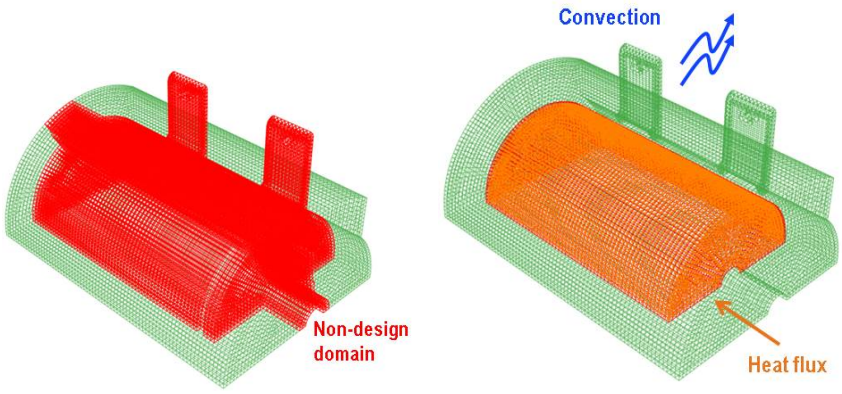

(a) (b)

Fig. 5: Geometric model and boundary conditions of an E-motor cover: (a) non-design domain (red color) and design domain (green color); (b) external heat flux applied at the inner wall and convection defined over the structural boundary.

of 170mm and a radius of 70mm. It is discretized with a mesh consisting of 46574 linear hexahedral elements, 2522 linear wedge elements and 1474 linear tetrahedral elements. Other parameters are set as: $k = 0.385\text{W}/(\text{mm} \cdot \text{K})$, $h = 2\times10^{-5}\text{W}/(\text{mm}^2\cdot\text{K})$ and $T_{ref} = 20^oC$. The design problem is to minimize the thermal compliance subject to a volume constraint of 50% of the entire structure, including both design and non-design domains.

Table 3: Validation value of E-motor cover designs

	Average Temp. at Flux Region (°C)	Max. Temp. (°C)	Min. Temp. (°C)	Volume
Design I	219	227	179	50.4%
Design II	228	235	214	49.5%

By applying casting constraints along the radial direction of the motor's central axis, two conceptual design proposals with different minimum member sizes are presented in Figs. 6 and 7, respectively. For comparison, the optimized density distribution, the corresponding smoothed design, the verification results showing the temperature distribution and the convergence curves are given for both designs. The first design as shown in Fig. 6 is obtained by applying a minimum-member-size restriction of 10mm. For such a design, spike-shape structures appear over the electric motor cover in order to effectively transfer the heat to the environment. By enlarging the minimum length scale to 20mm, thicker wall structures are observed in the optimized design as shown in Fig. 7. The detailed verification results for average temperature at the flux region as well as the maximum and the minimum temperature over the structure are recorded in Tab. 3. The verification reveals as expected that the design with a smaller member size achieves a better heat transferring capability compared to the other, though the volume ratios of two verification models are slightly different.

3.2.2 Optimized designs with different material and convection coefficients

For the combined conductive and convective heat transfer problems, the dimensionless Biot number $B = \frac{h \cdot L_c}{k}$, where L_c is a reference length, quantifies the ratio of heat transfer resistances at the surface and inside of a structural body. For topology optimization of such a problem, different Biot numbers will result in different optimized structural layouts (Alexandersen (2011a,b); Coffin and Maute (2015)). Generally, a high B value leads to a design with pronounced structural features, such as elongated thin arms for which the planner surface area is maximized for an efficient heat dissipation through convection. In contrast, a low B value usually results in an optimized design with material accumulating near the heat source. Such phenomena are reproduced here by designing the E-motor cover with copper and steel using different convections. Fig. 8 compares two design proposals, where Fig. 8(a) is the same as that in Fig. 6 with $k = 0.385\text{W}/(\text{mm} \cdot \text{K})$, $h = 2 \times 10^{-5}\text{W}/(\text{mm}^2 \cdot \text{K})$ and Fig. 8(b) is obtained with a lower conductivity $k = 0.065\text{W}/(\text{mm} \cdot \text{K})$ and a higher convection coefficient $h = 5 \times 10^{-3}\text{W}/(\text{mm}^2 \cdot \text{K})$. For the latter case with a high B value, the conductive material accumulates around the heat source of the E-motor cover in layers of fins along its central axis. Note, that both optimization processes are executed for the same volume fraction and with the same

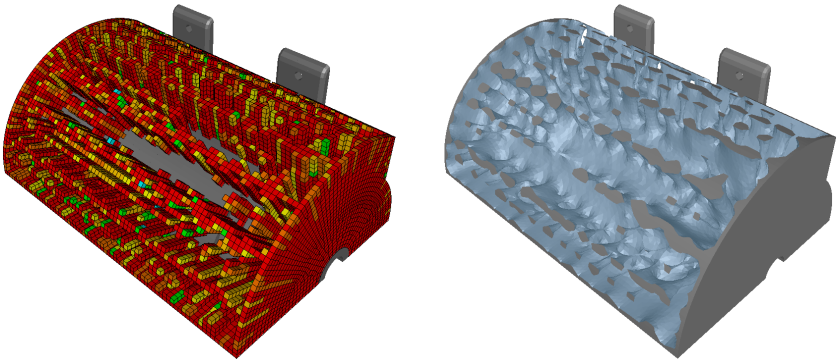

(a) (b)

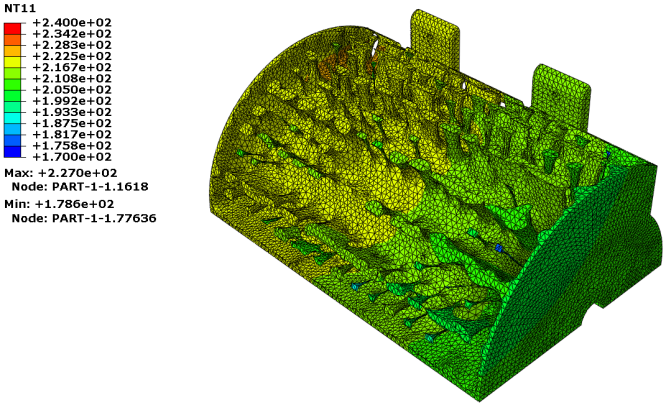

(c)

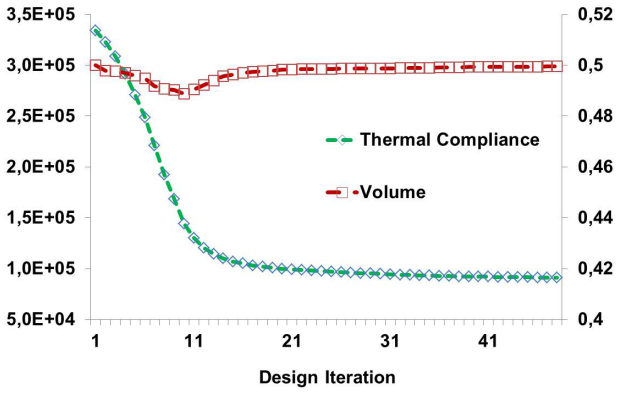

(d)

Fig. 6: Topological design I of an E-motor cover for a small minimum member size: (a) density distribution; (b) smoothed design; (c) temperature distribution; (d) convergence curve.

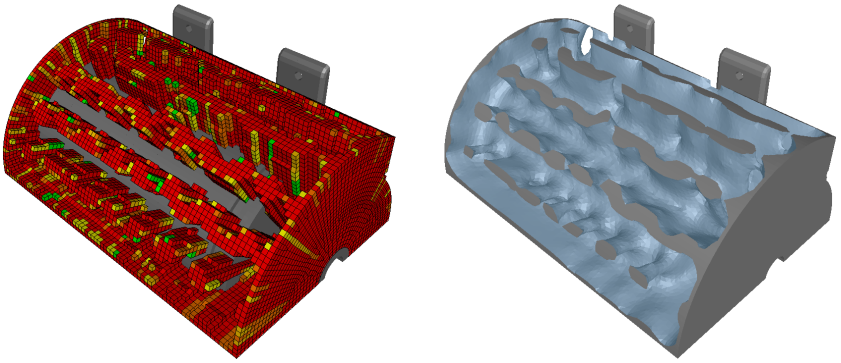

(a) (b)

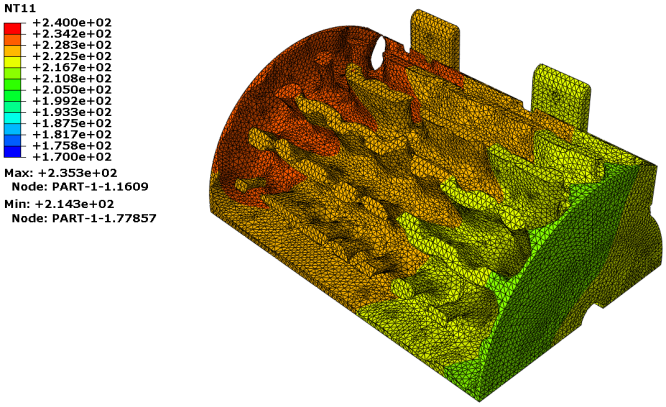

(c)

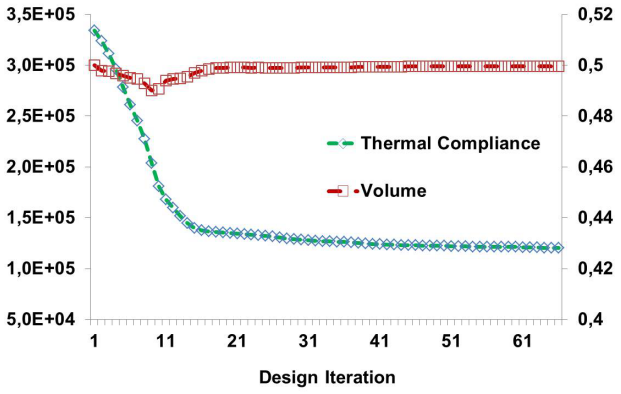

(d)

Fig. 7: Topological design II of an E-motor cover for a large minimum member size: (a) density distribution; (b) smoothed design; (c) temperature distribution; (d) convergence curve.

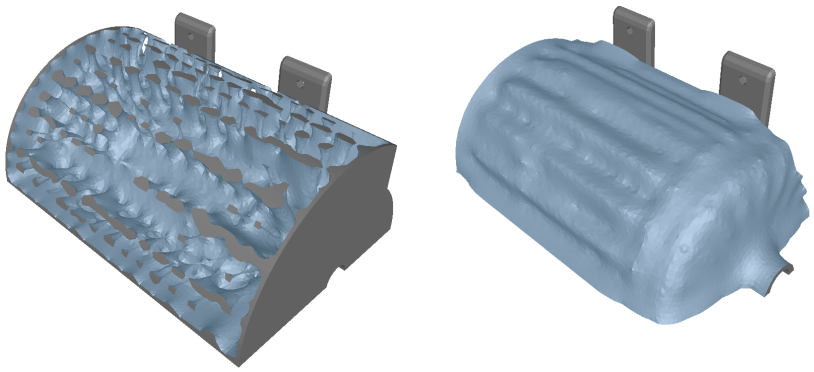

(a) (b)

Fig. 8: Topological design of E-motor cover with different ratios of convection coefficient and thermal conductivity: (a) $B = 0.9 \times 10^{-2}$ and (b) $B = 13.1$.

minimum member size. The length of the E-motor cover is used as the reference length $L_c = 170$mm for calculating the Boit numbers. The optimization results here are in an agreement with the previous studies in (Alexandersen (2011a,b); Coffin and Maute (2015)). Readers are referred to the references therein for further discussions on the impact of applying different materials and convection coefficients in topology optimization.

3.3 Topological design of heat sinks

3.3.1 Optimization with thermal and static design responses

Heat sinks are passive heat exchangers that are used widely in electronic devices to cool key components such as central processing unit (CPU) or graphics cards in a computer. In this section, several heat-sink designs for a CPU are presented by using topology optimization and their thermal and static performance are compared. The initial geometry and boundary conditions are given in Fig. 9. It consists of a design domain (the upper cubic part) of dimension $100 \times 100 \times 50$mm and a non-design domain (the bottom base) of dimension $40 \times 40 \times 10$mm for assembly purpose. A uniform surface heat flux of magnitude 0.1W/mm^2 is applied at the bottom surface and a forced convection exists over the structural boundaries. The optimization problem is to minimize the thermal compliance s.t. a volume constraint of 30% of the initial geometry. The model is discretized into 72000 linear hexahedral elements for finite analysis. For the solid material, the Young's modulus of 70GPa, the density of $2.8 \times 10^{-6}\text{kg/mm}^3$ and the Possion ratio of 0.35 are assumed. Other parameters are set as follows: $k = 0.237\text{W/(mm} \cdot \text{K)}$, $h = 1 \times 10^{-4}\text{W/(mm}^2 \cdot \text{K)}$ and $T_{ref} = 20^oC$.

Fig. 10 illustrates a reference heat sink design and the corresponding thermal and static simulation results. The sink possesses a desired mass fraction of 30% as specified. It has a fundamental structural frequency of 50.3Hz, an average temperature of 61.4^oC at the bottom surface, a maximum temperature of 62.2^oC and a minimum temperature of 44.1^oC. The detailed simulation results are recorded in Table. 5. For comparison, three other design proposals with the same volume fraction and a similar length scale are obtained using topology optimization.

Fig. 11 shows the first optimized heat sink (Design I) and its verification results. This design is obtained by applying three manufacturing constraints (extrusion, casting and symmetry) in the topology optimization process. The direction of the extrusion is out of plane and the casting direction is in the 45-degree direction on each half of the structure. The overall design process converges in 26 design iterations with an active volume constraint. The second design proposal (Design II) is given in Fig. 12, which is obtained by applying one symmetry constraint and one casting constraint in the upward direction normal to the base. This design possesses spikes and thin-walled structures which follow the casting direction and spread over the base. The optimization process takes 28 design iterations to converge with an active volume constraint.

To evaluate the performance difference between the density model and the final CAD design, the optimization value of Designs I and II from SIMULIA-Tosca are recorded in Table. 4. Note, that the minimum temperature in the design domain appears in the void region, which equals to the ambient reference temperature. Comparing to Table. 5, the verification results slightly differ from the optimization value as shown in Table. 4 for several reasons. First, design-dependent convection coefficients are assumed inside the design domain in optimization, while in verification a constant convection coefficient is considered over the structural surface of a solid-void CAD model. Second, the verification model (CAD model) deviates from the density model after the iso-surface extraction, smoothing and local surface modifications. The differences on the volume fraction between the verification and optimization models are feasible from an engineering point of view. In this example, Design II exhibits a better heat transfer capability as its average temperature at the flux regions is lower than that of Design I. Besides, as a by-product of this optimization, the maximum temperature of Design II is also lower than that of Design I.

In practice, it is common to have both static and thermal design requirements for the same design. Here, a third design proposal is obtained by maximizing the fundamental structural frequency of the heat sink subject to a thermal constraint that the maximum temperature of the heat sink must not exceed 60.0^oC. The volume fraction constraint and manufacturing restrictions are the same as those in Design I. Fig. 13 shows the smoothed design, the corresponding temperature distribution and the 1^{st} eigenmode shape. Comparing to Design I, this heat sink possesses shorter fins with major material accumulating around the base. It achieves a fundamental frequency of 147.9Hz and a maximum temperature of 73.6^oC in the post-processed design. Note, that

Table 4: Optimization value of heat-sink designs (Density model)

	Average Temp. at Flux Region (°C)	Max. Temp. (°C)	Min. Temp. (°C)	Volume
Design I	50.1	50.6	20.0	30.0%
Design II	48.9	49.4	20.0	30.0%

although in the optimization process the temperature constraint $T_{max} \leq 60^oC$ is strictly satisfied, the final temperature of the smooth result deviates from the constrained value by 22% due to the intermediate density in optimization and the postprocessing of the density model into solid-void CAD model by an iso-surface cut.

3.3.2 Verification with a thermo-fluidic model

The reference heat sink and optimized Design I in the previous section are further verified with thermo-fluid based conjugate heat transfer in COMSOL-Multiphysics (2015). As shown in Fig. 14(a), the heat sink is placed at the bottom of a computational domain, where a laminar air inflow of an average velocity rate 10.5m/s and initial temperature 20°C is applied from the left inlet to the right open boundary. The other four sides of the domain are assumed as walls with no fluid penetration. In addition, the material property of the heat sink and the external heat flux are the same as those in the previous verification using SIMULIA-Abaqus. In practice, the relation between the convection coefficient h and fluid velocity is affected by various factors, such as material properties, boundary conditions and part orientation which must be evaluated by experiments. Since the goal here is to demonstrate the design efficiency of the proposed design approach and solutions, the velocity of air is chosen based on an experimental study in Xiao et al (2011) for simplicity.

The steady-state fluid velocity and temperature distribution over the reference heat sink are given in Fig. 14(a-b) respectively. Furthermore, Fig. 15(a-b) shows the corresponding simulation results of the optimized design. Comparing to the verification results as shown in Figs. 10 and 11, which use a simplified convection model and a uniform ambient temperature, the temperature distribution over the heat sink here increases gradually in the direction of the fluid flow. The detailed thermal performance of two designs, including the average temperature at the flux region, the maximum and minimum temperature over the heat sink, are evaluated and listed in Tab. 6. Although the temperature values are different from those in previous section by using a different simulation model, the optimized Design I still exhibits a better thermal performance than the reference design. To this end, both verifications indicate that the proposed design optimization solution is able to yield efficient structural designs for combined conductive and convective heat transfer problems.

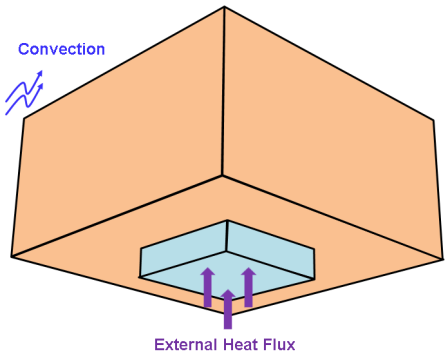

Fig. 9: Topology optimization of a passive heat sink: design domain (brown color), non-design domain (blue color) and boundary conditions.

Table 5: Verification of the smoothed heat-sink designs using a simplified engineering model

	Average Temp. at Flux Region (°C)	Max. Temp. (°C)	Min. Temp. (°C)	Volume	1^{st} Freq.(Hz)
Ref. Design	61.4	62.2	44.1	29.8%	50.3
Design I	56.6	57.2	42.8	29.2%	90.0
Design II	55.2	55.7	32.7	29.4%	70.7
Design III	73.0	73.6	58.2	30.3%	147.9

Table 6: Verification of the smoothed heat-sink designs using thermo-fluidic modeling

	Average Temp. at Flux Region (°C)	Max. Temp. (°C)	Min. Temp. (°C)	Volume
Ref. Design	43.6	45.4	22.3	29.8%
Design I	37.0	38.7	20.6	29.2%

4 Conclusions

An industrial solution for topology optimization of combined conductive and convective heat transfer problems is implemented in Dassault Systemes software solutions and numerical industrial experiments show promising results. The topology optimization feature is provided by SIMULIA.Tosca, where a simplified engineering model is utilized to model the design-dependent convection during the optimization process. Such a strategy allows for a seamless integration with the static-state heat simulation module in SIMULIA.Abaqus. Several design examples of different problem setups are given to demonstrate

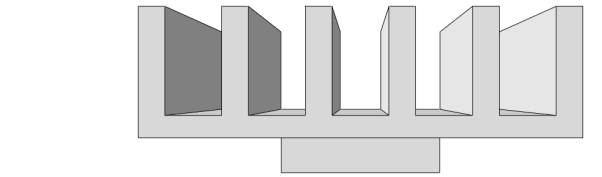

(a)

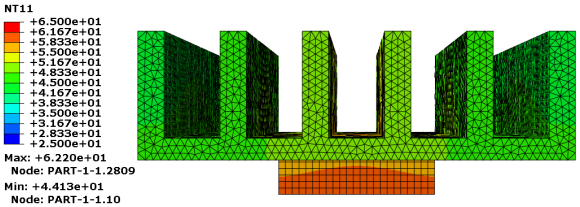

(b)

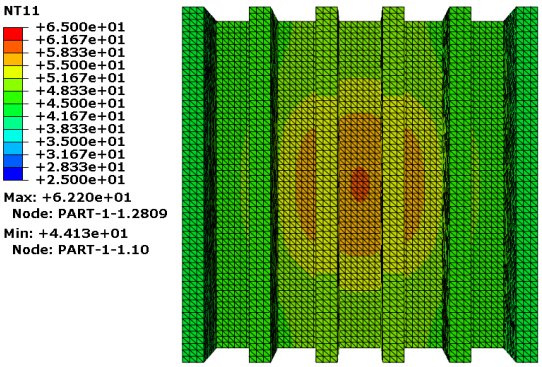

(c)

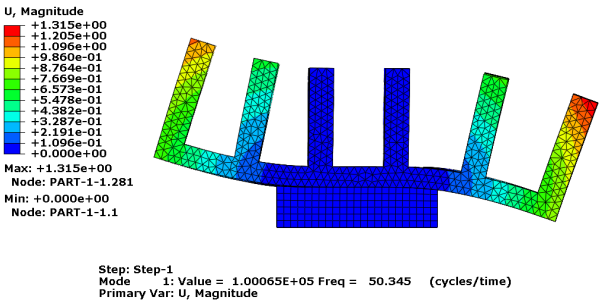

(d)

Fig. 10: A reference heat-sink design: (a) geometric model; (b,c) temperature distribution; (d) mode shape of 1^{st} eigenfrequency.

(a)

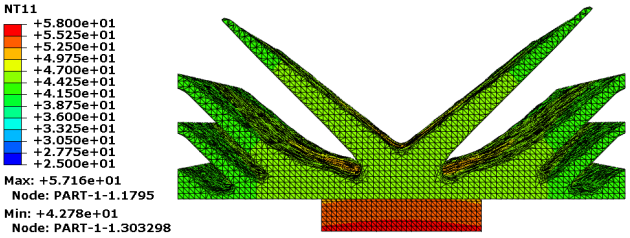

(b)

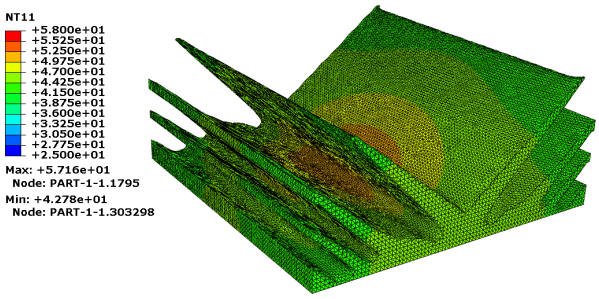

(c)

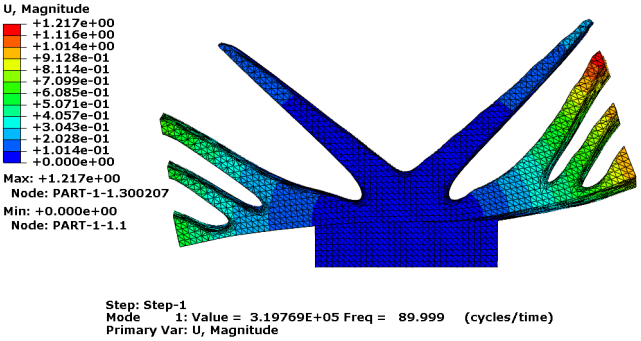

(d)

Fig. 11: Heat-sink design I: (a) smoothed design; (b,c) validation of temperature distribution; (d) mode shape of 1^{st} eigenfrequency.

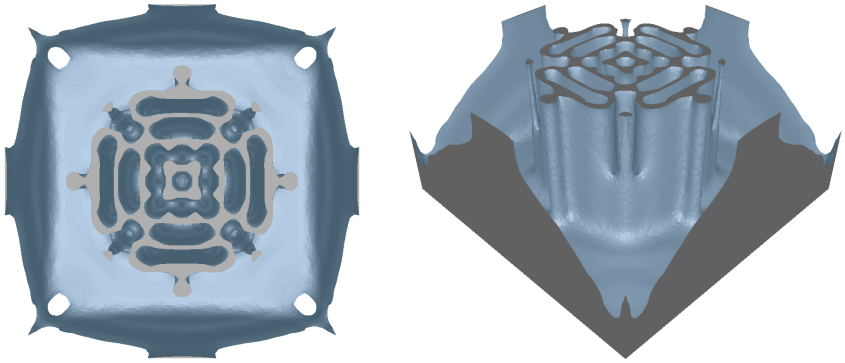

(a) (b)

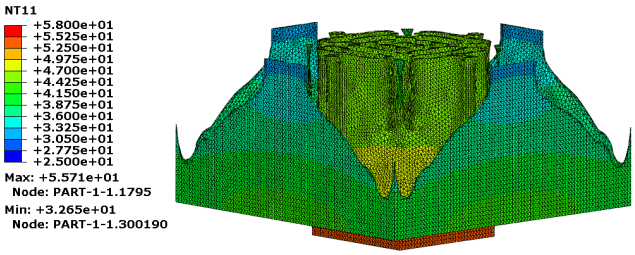

(c)

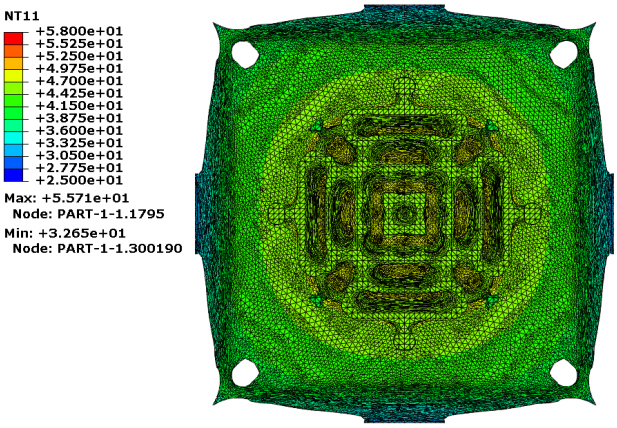

(d)

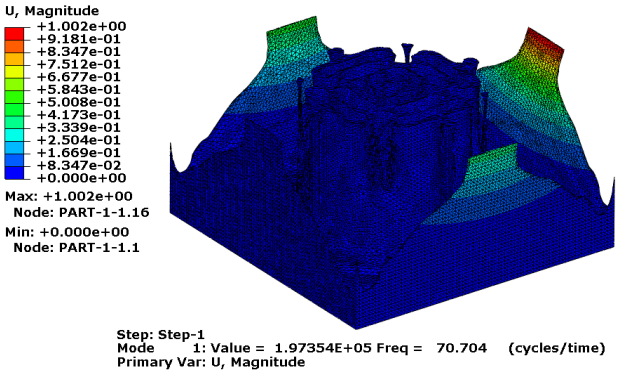

(e)

Fig. 12: Heat-sink design II: (a) smoothed design; (b,c) validation of temperature distribution; (d) mode shape of 1^{st} eigenfrequency.

(a)

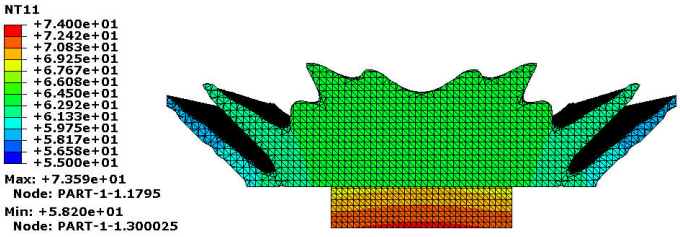

(b)

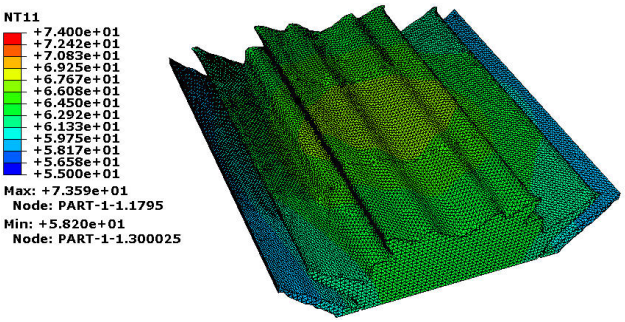

(c)

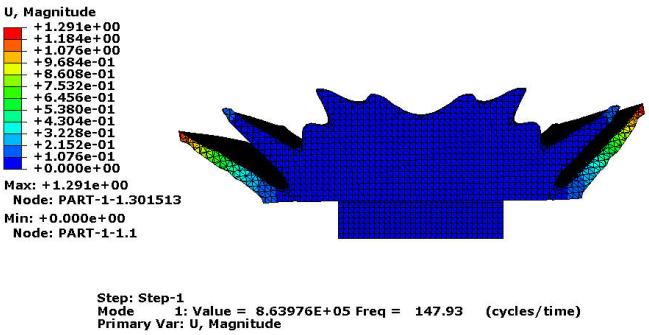

(d)

Fig. 13: Heat-sink design III: (a) optimized design; (b,c) temperature distribution; (d) mode shape of 1^{st} eigenfrequency.

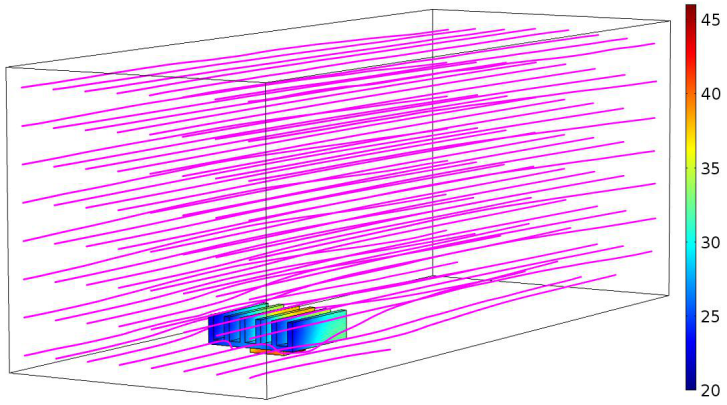

(a) simulation domain, flow streamline and temperature distribution (°C)

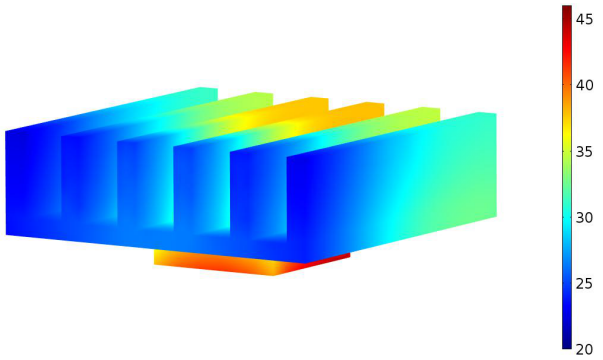

(b) temperature distribution over the heat sink (°C)

Fig. 14: Verification of the reference heat sink using thermo-fluidic modeling.

its applicability. Verification results of each optimized design are derived by either the steady-state heat transfer using the engineering convection scheme or the conjugate heat transfer with a thermo-fluidic model. Both studies indicate that the proposed solution is able to yield efficient design proposals for various practical design scenarios. Industrial applications can benefit from such a solution in designing topologically optimized structures with effective thermal management.

Acknowledgements The authors acknowledge the financial support received from the EU research project "LaScISO" (Large Scale Industrial Structural Optimisation), grant agreement No.: 285782, and from the research project "Sapere Aude TOpTEn" (Topology Optimization of Thermal ENergy systems) from the Danish Council for Independent

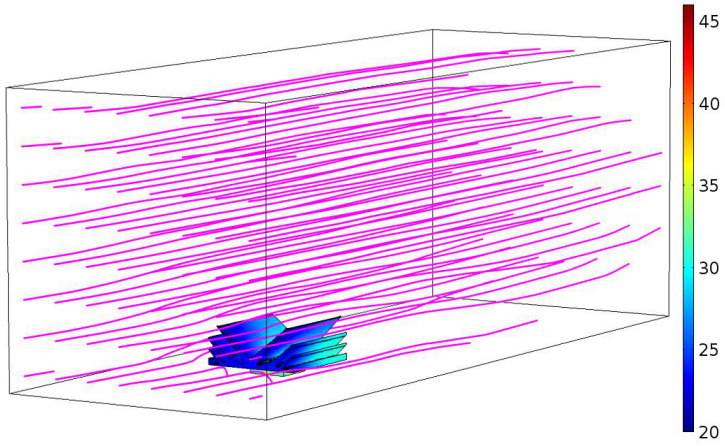

(a) simulation domain, flow streamline and temperature distribution (°C)

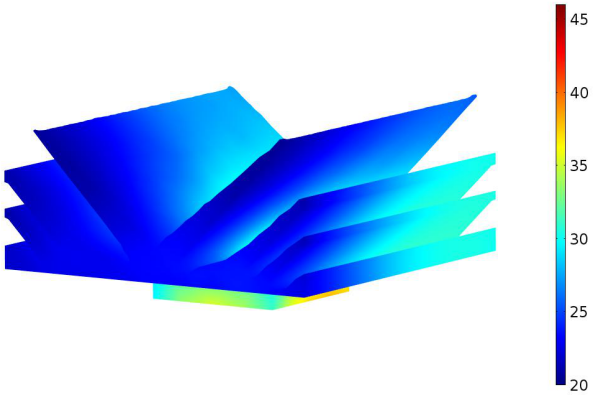

(b) temperature distribution over the heat sink (°C)

Fig. 15: Verification of heat-sink Design I using thermo-fluidic modeling.

Research, grant: DFF-4005-00320. The authors thank Daniel Kurfeß and Pratik Upadhyay from Dassault Systèmes Deutschland GmbH SIMULIA Office for the support in this project.

References

Ahn SH, Cho S (2010) Level set-based topological shape optimization of heat conduction problems considering design-dependent convection boundary. Numerical Heat Transfer, Part B: Fundamentals 58(5)(5):304–322, DOI 10.1080/10407790.2010.522869

Alexandersen J (2011a) Topology optimisation for axisymmetric convection problems. Tech. rep., Technical University of Denmark

Alexandersen J (2011b) Topology optimisation for convection problems - B.Eng. Thesis. Master's thesis, Technical University of Denmark, URL http://orbit.dtu.dk/en/publications/topology-optimization-for-convection-problems(2b27dfe6-a242-4849-8c8a-63d1e37792db).html

Alexandersen J, Aage N, Andreasen CS, Sigmund O (2014) Topology optimisation of natural convection problems. International Journal for Numerical Methods in Fluids 76 (10):699–721, DOI 10.1002/fld.3954

Bendsøe M, Kikuchi N (1988) Generating optimal topologies in structural design using a homogenization method. Comput Method Appl M 71:197–224

Bendsøe M, Sigmund O (2003) Topology Optimization - Theory, Methods and Applications. Spinger

Bruns T (2007) Topology optimization of convection-dominated, steady-state heat transfer problems. International Journal of Heat and Mass Transfer 50(15-16):2859–2873, DOI 10.1016/j.ijheatmasstransfer.2007.01.039

Coffin P, Maute K (2015) Level set topology optimization of cooling and heat devices using a simplified convection model. under review in Structural and Multidisciplinary Optimization

COMSOL-Multiphysics (2015) Version 5-1 COMSOL, Inc

Dede E, Joshi SN, Zhou F (2015) Topology optimization, additive layer manufacturing, and experimental testing of an air-cooled heat sink. ASME Journal of Mechanical Design (available online), DOI 10.1115/1.4030989

Iga A, Nishiwaki S, Izui K, Yoshimura M (2009) Topology optimization for thermal conductors considering design-dependent effects, including heat conduction and convection. International Journal of Heat and Mass Transfer 52(11-12):2721–2732, DOI 10.1016/j.ijheatmasstransfer.2008.12.013

Sigmund O (2001) Design of multiphysics actuators using topology optimization part i: One-material structures. Comput Method Appl M 190:6577–6604, DOI 10.1016/S0045-7825(01)00251-1

SIMULIA-Abaqus (2015) Manual, Dassault Systèmes Simulia

SIMULIA-Tosca (2015) Manual, Dassault Systèmes Simulia

Xiao B, Wang G, Wang Q, Maniruzzaman M, Jr RDS, Rong Y (2011) An experimental study of heat transfer during forced air convection. JMEPEG 20:1264–1270, DOI 10.1007/s11665-010-9745-7

Yin L, Ananthasuresh G (2002) A novel topology design scheme for the multiphysics problems of electro-thermally actuated compliant micromechanisms. Sensors and Actuators 97-98:599–609, DOI 10.1016/S0924-4247(01)00853-6

Yoon GH (2010) Topological design of heat dissipating structure with forced convective heat transfer. Journal of Mechanical Science and Technology 24(6):1225–1233, DOI 10.1007/s12206-010-0328-1

Yoon GH, Kim YY (2005) The element connectivity parameterization formulation for the topology design optimization of multiphysics systems. International Journal for Numerical Methods in Engineering 64(12):1649–1677, DOI 10.1002/nme.1422